Hydrology and Earth System Sciences Discussions

Uncertainties on mean areal precipitation: assessment and impact on streamflow simulations

L. Moulin[1,2], E. Gaume[1,3], and C. Obled[4]

[1]Université Paris-Est, Cereve, UMR – MA102 Agroparistech, 77455 Marne la Vallee 2, France
[2]UPMC Univ Paris 06, UMR 7619 Sisyphe, 75005 Paris, France
[3]Lab Cent Ponts & Chaussees, 44341 Bouguenais, France
[4]Inst Natl Polytech Grenoble, Lab Etud Transferts Hydrol & Environm, BP 53,
38041 Grenoble 9, France

HESSD

5, 2067–2110, 2008

Impact on streamflow simulations of uncertainties on MAP

L. Moulin et al.

Title Page

Abstract	Introduction
Conclusions	References
Tables	Figures

|◄ | ►|
◄ | ►

Back | Close

Full Screen / Esc

Printer-friendly Version

Interactive Discussion

Abstract

This paper investigates the influence of mean areal rainfall estimation errors on a specific case study: the use of lumped conceptual rainfall-runoff models to simulate the flood hydrographs of three small to medium-sized catchments of the upper Loire river. This area (3200 km^2) is densely covered by an operational network of stream and rain gauges. It is frequently exposed to flash floods and the improvement of flood forecasting models is then a crucial concern. Particular attention has been drawn to the development of an error model for rainfall estimation consistent with data in order to produce realistic streamflow simulation uncertainty ranges. The proposed error model combines geostatistical tools based on kriging and an autoregressive model to account for temporal dependence of errors. It has been calibrated and partly validated for hourly mean areal precipitation rates. Simulated error scenarios were propagated into two calibrated rainfall-runoff models using Monte Carlo simulations. Three catchments with areas ranging from 60 to 3200 km^2 were tested to reveal any possible links between the sensitivity of the model outputs to rainfall estimation errors and the size of the catchment. The results show that a large part of the rainfall-runoff (RR) modelling errors can be explained by the uncertainties on rainfall estimates, especially in the case of smaller catchments. These errors are a major factor limiting accuracy and sharpness of rainfall-runoff simulations, and thus their operational use for flood forecasting.

1 Introduction

Despite decades of developments and testing, rainfall-runoff (RR) models are still seldom used by operational flood forecasting services. This is particularly true in flash-flood prone areas where accurate RR simulations would yet be necessary to compute short lead-time forecasts. The lack of accuracy and robustness of RR models, while not striking (see Andreassian et al., 2006, for a review of models and performances), remains critical for some applications.

HESSD

5, 2067–2110, 2008

Impact on streamflow simulations of uncertainties on MAP

L. Moulin et al.

Title Page

Abstract | Introduction

Conclusions | References

Tables | Figures

◀ | ▶

◀ | ▶

Back | Close

Full Screen / Esc

Printer-friendly Version

Interactive Discussion

This arises the question of the sources of uncertainties affecting RR simulations: what are the major factors limiting the accuracy of RR simulations? On which ones a particular attention has to be drawn? Is there any possibility of improvement of simulations? A better insight into these questions is necessary to give some orientations to future research works on RR modelling. It will also improve the assessment of the capabilities and limits of the existing models.

Among the various sources of uncertainty affecting RR modelling (Melching, 1995), uncertainties on computed precipitations play a particular role (Sun et al., 2000; Bardossy and Das, 2008). Rainfall rates are the main input data of RR models and, in that sense, are one of the first factors controlling the accuracy of RR simulations. The general issue of the impact of rainfall inputs on RR simulation accuracy encompasses at least two main questions:

- the level of spatial and temporal discretisation needed to represent accurately the RR processes dynamics in the hydrological models, generally assessed through sensitivity analyses (Michaud and Sorooshian, 1994; Vischel and Lebel, 2007; Segond et al., 2007),

- the assessment of the intrinsic quality of the mean areal precipitation (MAP) estimated over the whole considered catchment in the case of lumped RR models (or over each of the sub-units defined in distributed models); and then the assessment of its consequences on RR simulations.

The first question is linked to the debate about the relative merits of distributed versus lumped hydrological models. It is not the focus of this paper but will be mentioned in the conclusion section. The answer to the second question depends on the rainfall measuring techniques. The weather radar coverage has dramatically increased over the last decades giving access to measurements at high spatial and temporal resolutions. The radar signal treatment methods have significantly been improved (Krajewski and Smith, 2002; Gourley and Vieux, 2006; Chapon et al., 2008). However, quantitative precipitation estimates still present difficulty. Research works are ongoing to evaluate

Impact on streamflow simulations of uncertainties on MAP

L. Moulin et al.

radar rainfall estimation errors and the suitability of radar data for hydrological applications (Carpenter et al., 2001; Borga, 2002; Carpenter and Georgakakos, 2004; Borga et al., 2006; Cole and Moore, 2008). But in many cases, quantitative precipitation estimates used as input of hydrological models and especially flood forecasting models still rely on raingauge measurements. It is especially the case for the upper Loire area, the selected study area, where due to implementation problems, no quantitative precipitation estimates can be retrieved from the radar data. The question of the assessment of the uncertainties of MAP estimated through raingauge measurements is therefore remaining active. Moreover, an accurate assessment of both the associated uncertainties and their impact on RR simulations would define a reference state to evaluate the gains due to improvements of rainfall measurement techniques.

When raingauge data are used to estimate MAP, the major source of input uncertainty comes from the lack of representativeness of a discrete set of gauges of a network (Dulal et al., 2006; Refsgaard et al., 2006; Rode and Suhr, 2007; Villarini et al., 2008) and from the necessity to interpolate the rain rates between these points. Beyond the acknowledgment of the importance of MAP estimation uncertainties, a detailed assessment of their possible impact on the RR simulations has two main practical objectives:

– To evaluate the possible gains that could be obtained through an improvement of the rainfall measuring techniques especially the radar system.

– To determine the rainfall estimation uncertainty level to be able to turn from the standard deterministic hydrological forecasting approach (disappointing since it frequently fails to deliver correct forecasts), to a stochastic approach taking into account all the possible streamflow evolutions given the uncertainties about actual rainfall amounts.

Most of the previous studies on MAP uncertainty propagation in RR models were either empirical or purely theoretical sensitivity analyses. Empirical analyses are generally based on the comparison of various interpolation approaches (Creutin and Obled,

1982; Lebel et al., 1987; Johansson, 2000) or based on under-sampling of relatively dense raingauge networks (Anctil et al., 2006; Balme et al., 2006; Bardossy and Das, 2008). Theoretical analyses are based on an a priori chosen error model to corrupt the computed MAPs (Xu and Vandewiele, 1994; Paturel et al., 1995; Nandakumar and Mein, 1997; Carpenter and Georgakakos, 2004; Oudin et al., 2006). In that case, no validation of the error model is processed to ensure consistency with the available data.

The main contribution of the present work is the effort done to build, calibrate and validate a realistic error model on MAP estimates. The hereafter presented developments around the definition and validation of a rainfall estimation error model may appear sophisticated. This sophistication is nevertheless not a scientific gadget: the realism of the error model is a necessary condition to draw any valuable conclusion from the propagation of these errors into RR models. Inspired by the methodology used by Storm et al. (1989) and Datin (1998), the proposed approach relies on geostatistical tools. The selected method for evaluating MAP errors and their impact on the simulated streamflows is composed of three steps.

1. Calibration and validation of an hourly rainfall interpolation error model.

2. Calibration and validation of a temporal dependence model for these errors to be able to produce realistic hourly MAP error series.

3. Use of Monte Carlo simulations of rainfall scenarios based on the calibrated error model and propagation of these scenarios into two selected lumped RR models.

The selected RR models are modified versions of the GR4J model (Perrin et al., 2003) and of TOPMODEL (Beven and Kirby, 1979; Mathevet, 2005). Various catchment areas are considered to reveal a possible link between the sensitivity to MAP uncertainties and the considered catchment area.

The paper is structured as follows. The study area and data sets are presented in Sect. 2. The interpolation method and principles of the proposed error model are exposed in Sect. 3. The cross-validation approach and the obtained error model validation results are presented in Sect. 4. Section 5 is devoted both to the propagation

Printer-friendly Version

Interactive Discussion

of the MAP errors into the RR models and to the interpretation and discussion of the obtained results. Conclusions from the study are summarised in Sect. 6.

2 The study area and data

The upper Loire River is located in the northern part of the Cevennes-Vivarais Hydro-Meteorological Observatory region (Delrieu, 2003; Delrieu et al., 2005). The catchment of the upper Loire River at Bas-en-Basset covers 3234 km^2 (Fig. 1). It is an upland, mainly rural area with dominantly plutonic, metamorphic and locally volcanic bedrocks. The soils are relatively shallow (from a few centimeters to a few meters, on average less than one meter deep). The elevation of the catchment ranges from about 450 to 1700 m a.s.l.

The study area is exposed to various climatic influences. Mediterranean storms induce flash-floods that affect headwater catchments in the south-eastern part of the area. This explains the very high 10-year flood specific flow values of these catchments, which range from 0.4 to 5.6 m^3 s^{-1} km^{-2} (Table 1). Conversely, the north-western part of the upper Loire river basin is influenced by a typical oceanic climate, with moderate flood events. Due to the altitudes and the mid-mountain climatic influence, snowfall and snowmelt may sometimes be non negligible elements of the water budget in the south-eastern part of the upper Loire. Nevertheless, they have little influence on the major flood events that predominantly occur in autumn and which are here the main concern. Consequently, in this study, no snowmelt routine is implemented in the tested RR models.

The density of the raingauge network has progressively increased over the years: the number of automatic raingauges has grown from six in 1977 to 40 at present. The automatic raingauge network now in operation, developed for flash flood forecasting purposes, is relatively dense (about 1/80 km^2) if compared to the average density of automatic raingauges in France (1/500 km^2). Moreover, the upper Loire hydrologic network of rain and stream gauges is considered to be among the best-maintained

Title Page

Abstract	Introduction
Conclusions	References
Tables	Figures

◄	►
◄	►
Back	Close

Full Screen / Esc

Printer-friendly Version

Interactive Discussion

operational networks in France. A weather radar system, located in the North-West of the upper Loire catchment, has been in operation since 1996. But due to technical problems, such as the high elevation of the radar (1116 m a.s.l.), ground clutter, and masking effects caused by the surrounding trees and topography of the region, it has not yet been possible to use weather radar to estimate rainfall rates. Mean areal precipitation (MAP) estimations can therefore only rely on the raingauge network.

Three nested catchments have been selected for this study. This choice has been dictated by the quality and length of the available streamflows series (20 years for Rieutord, 27 years for both Chambon-sur-Lignon and Bas-en-Basset), their location in areas affected by flash floods, and the desire to cover a large range of catchment surfaces (62, 139, and 3234 km^2). Some intermediate-sized catchments are available but affected by dam management. The main characteristics of these three catchments are summarised in Table 1.

3   Methodology for estimating precipitation uncertainties

3.1   A geostatistical framework

Geostatistical methods and especially kriging are now generally accepted as the most effective approaches to interpolate point rainfall measurements. They have been widely used and tested in the past and appear to deliver reasonable rainfall estimates, particularly in the case of sparse networks (Lebel et al., 1987; Haberlandt, 2007).

Kriging is basically a linear interpolation approach. The estimated values of point rainfall amounts $P_t(x_0)$ at any location x_0 as well as mean areal precipitation $\text{MAP}_t(S)$ over a given domain S are, at any time t, considered as linear combinations of the point rainfall amounts $P_{t,j}$ measured by the raingauges of the surrounding raingauge

network (Eqs. 1 and 2):

$$P_t(x_0) = \sum_{j=1}^{n} \mu_{t,j} P_{t,j} + \varepsilon_t(x_0) \tag{1}$$

$$\mathrm{MAP}_t(S) = \sum_{j=1}^{n} \lambda_{t,j} P_{t,j} + \varepsilon_t(S) \tag{2}$$

with n the number of the considered raingauges, $\varepsilon_t(x_0)$ and $\varepsilon_t(S)$ the estimation errors on $P_t(x_0)$ and $\mathrm{MAP}_t(S)$. The value of the weights $\mu_{t,j}$ and $\lambda_{t,j}$ are adjusted to minimise the variance of the errors $\varepsilon_t(x_0)$ and $\varepsilon_t(S)$ given some assumptions concerning the spatial structure of the rainfall fields. Kriging is flexible in the sense that a large variety of hypotheses about this spatial structure can be accounted for: observed anisotropy of rainfall fields, general trends linked to the relief for instance, spatial rainfall structure varying with seasons or rainfall types, etc. Nevertheless, ordinary kriging assumptions are generally selected for interpolating rainfall rate fields (Chen et al., 2008), especially when small time steps are considered. Moreover, accounting for anisotropy (Lebel et al., 1987; Haberlandt, 2007) or trends (Kieffer-Weisse and Bois, 2002) does generally not show to improve significantly the interpolation accuracy, in particular in the case of short time steps. Therefore, the following assumptions were done for the interpolation model presented herein: (a) the spatial correlation structure (normalised variogram or correlogram) is the same for every time step and rainfall events (climatological kriging), (b) the variogram is isotropic, (c) the possible influence of altitude and exposition is neglected for the interpolation (i.e. the interpolation is only based on inter-distances), (d) a spherical variogram (Eq. 3) is used.

$$\gamma(h, \alpha, \beta) = \begin{cases} \alpha \cdot \left[\dfrac{3}{2} \cdot \dfrac{h}{\beta} - \dfrac{1}{2} \cdot \left(\dfrac{h}{\beta} \right)^3 \right] & h \le \beta \\ \alpha & h > \beta \end{cases} \tag{3}$$

Impact on streamflow simulations of uncertainties on MAP

L. Moulin et al.

Title Page

Abstract	Introduction
Conclusions	References
Tables	Figures

◄◄ ►►

◄ ►

Back Close

Full Screen / Esc

Printer-friendly Version

Interactive Discussion

where γ is the semi-variogram, h is the distance between two locations (inter-distance), α is the sill (equal to unity in the case of climatological kriging, given the normalisation with rainfall field standard deviation) and β is the range of the variogram (in km).

The main adjustment factor of this kriging model is the variogram shape and particularly its range β. Previous works conducted in the same region (Lebel et al., 1987) led to the calibration of a relation between the time step considered and the range β for a spherical variogram (Eq. 4). According to this relationship, the range of the variogram of hourly rain rates is set equal to 25 km.

$$\beta(\text{km}) = 25\Delta t^{0.3} \tag{4}$$

where β is the range (in km) and Δt is the time step (in hours) of the rainfall data. This estimate of range appears to be well suited to the upper Loire river area when plotting empirical variograms for heavy rainfall events (convective).

3.2 The rainfall interpolation errors and the error model

3.2.1 Model for interpolation errors

Interpolation models based on kriging deliver not only interpolated values but also an estimate of the associated uncertainty through the computation of a theoretical interpolation error variance σ^2 or a standard deviation σ, also named kriging standard deviation (Eqs. 5 and 6).

$$\sigma_t^2(x_0) = E\{\varepsilon_t(x_0)^2\} \tag{5}$$

$$\sigma_t^2(S) = E\{\varepsilon_t(S)^2\} \tag{6}$$

When a climatological variogram $\bar{\gamma}_{ij}$ between points x_i and x_j (inter-distance d_{ij}) is used, the weights $\mu_{t,j}$ and $\lambda_{t,j}$ are supposed constant over the time if the raingauge network remains unchanged. The kriging interpolation errors may then be normalised

HESSD

5, 2067–2110, 2008

Impact on streamflow simulations of uncertainties on MAP

L. Moulin et al.

Title Page

Abstract | Introduction

Conclusions | References

Tables | Figures

|◄ | ►|

◄ | ►

Back | Close

Full Screen / Esc

Printer-friendly Version

Interactive Discussion

by the standard deviation of rainfall field SD_t. The resulting normalised standard deviation $\bar{\sigma}_t$ depends then only on the topology on the raingauge network, i.e. on the configuration (distance, direction) and on the numbers of the surrounding raingauges. Thus it may be constant over several time steps (Lebel et al., 1987) and constant over the whole period in case of a stationnary network (no evolution of network and no failure in data collection).

$$\bar{\sigma}(x_0) = \sigma_t(x_0)/SD_t \tag{7}$$

$$\bar{\sigma}(S) = \sigma_t(S)/SD_t \tag{8}$$

Errors $\bar{\sigma}(x_0)$ and $\bar{\sigma}(S)$ (Eqs. 7 and 8) can be minimised by the method of Lagrange multipliers. The values $\xi(x_0)$ and $\xi(S)$ are used to impose unbiased rainfall estimates: $\sum_{i=1}^{n} \mu_i = 1$ and $\sum_{i=1}^{n} \lambda_i = 1$ (Eqs. 9 and 10).

$$\xi(x_0) = \bar{\gamma}_{i0} - \sum_{j=1}^{n} \mu_i \bar{\gamma}_{ij}, \ \forall i \tag{9}$$

$$\xi(S) = \bar{\gamma}_{iS} - \sum_{j=1}^{n} \lambda_j \bar{\gamma}_{ij}, \ \forall i \tag{10}$$

with $\bar{\gamma}_{i,0}$ the normalised semi-variogram function depending on the distance h between the locations i and j, $\bar{\gamma}_{iS}$ the average value of the semivariogram between the raingauge x_i and any point of the surface S (Eq. 11) and $\bar{\gamma}_{SS}$ the average value of the semivariogram between the points of the surface S (Eq. 12).

$$\bar{\gamma}_{iS} = \frac{1}{S} \int_S \bar{\gamma}(x_i - x) \, dx \tag{11}$$

$$\bar{\gamma}_{SS} = \frac{1}{S^2} \int_S \int_S \bar{\gamma}(x - x') \, dx \, dx' \tag{12}$$

Title Page

Abstract | Introduction

Conclusions | References

Tables | Figures

◄ | ►

◄ | ►

Back | Close

Full Screen / Esc

Printer-friendly Version

Interactive Discussion

This ordinary kriging method with a climatological variogram yields:

$$\bar{\sigma}(x_0) = \sum_{i=1}^{n} \mu_i \bar{\gamma}_{i,0} + \xi(x_o) \tag{13}$$

$$\bar{\sigma}(S) = \sum_{i=1}^{n} \lambda_i \bar{\gamma}_{i,S} - \bar{\gamma}_{SS} + \xi(S) \tag{14}$$

The model for normalised interpolation errors proposed here assumes that these errors in estimates of both point and areal hourly precipitations, follow a zero-mean Gaussian distribution whose standard deviation is $\bar{\sigma}_t$ (depending on the available rain gauge network at time t). A normalised standard deviation $\bar{\sigma}(x_0)$ (resp. $\bar{\sigma}(S)$) lower than 0.5 means that more than 75% of rainfall field variance at the location x_0 (resp. on the area) is explained (kriging standard deviation = 0.5; then kriging variance = 0.5^2=0.25; explained variance = 1–0.25=0.75). When it is lower than 0.7, more than 50% of the observed signal is explained.

In Fig. 2, the distribution of theoretical normalised kriging standard deviation $\bar{\sigma}(x_0)$ for point estimates is mapped for interpolated daily and hourly rainfall rates for the upper Loire river catchment with the available network in the year 2003. It appears that for hourly rain rates, the theoretical point kriging standard deviation is higher than 0.7 on more than 50% of the study area. In other words, the spatial interpolation explains less than 50% of the variance of the observed signal on more than half of the area.

Likewise, Fig. 3 shows the evolution over time of the proportion of the upper Loire area where $\bar{\sigma}(x_0)$ for point rainfall estimates is lower than 0.5 or 0.7 (more than 75% or 50% of the variance of the signal is explained). Despite the increase of the density of the raingauge network for the last 20 years, from 1 tipping bucket raingauge for 500 km^2 to 1 for 80 km^2, high uncertainties remain on point rainfall rates estimated through spatial interpolation in many parts of the region, especially when short time steps are considered (hourly rainfall rates). In other words, poor or even no information on the hourly rain rates is available on the majority of the area. Nevertheless, the situation

for MAP estimation uncertainties is generally less dramatic due to averaging especially when large time steps and/or large areas are considered (Villarini et al., 2008). For instance, in year 2003, the kriging standard deviation of MAP $\bar{\sigma}(S)$ with all raingauge available is 0.15 for the MAP computed on the catchment of Loire at Bas-en-Basset,
5 0.24 for catchment at Chambon-sur-Lignon and 0.32 at Rieutord.

3.2.2 Modelling temporal structure of interpolation errors

Possible time dependence between successive interpolation errors must be considered in an error model to produce realistic error time series. At a given time, interpolation errors are due to the spatial sampling that may not capture some features of the rainfall
10 field: typically over or under-estimations linked to the relative position of intense rainfall cells and raingauges. If the time step is short according to the displacement of the cells, the same type of error may affect several successive estimates. Interpolation errors for both point and areal estimates may be dependent in time.

  The dependence in time between hourly rain rate interpolation errors will be analysed
15 using the available raingauge measurements. Raingauges are removed in turn from the network and the rainfall intensities computed at the corresponding location using the remaining network (cross validation detailed in Sect. 4.1). The comparison of the measured and computed intensities delivers series of hourly point rainfall estimation errors. The temporal structure of these series can be then examined and simulated.

20 A linear autoregressive model has been first tested to reproduce the observed dependence in time between these errors (Eq. 15).

$$\eta_{t+1} = \rho \cdot \eta_t + \sqrt{(1 - \rho^2)} \cdot \bar{\sigma}_t \cdot v_{t+1} \tag{15}$$

where η_t is the normalised interpolation error at time step t, ρ is the autocorrelation coefficient between two successive errors, $\bar{\sigma}_t$ is the theoretical standard deviation of the
25 interpolation normalised error distribution and v_{t+1} a random variable with a standard normal distribution.

This model will be calibrated, tested and validated for point rainfall estimates. Without reference values for MAPs, it is not possible to conduct the same tests and validations for the errors on MAPs. As for the spatial interpolation model, the evaluation of its adequacy can only rely on point rainfall validation.

Due to the linearity of both the kriging interpolation model and the autoregressive (AR) model, the selected AR model for point rainfall errors will also hold for MAP errors provided that its parameters – i.e. the autocorrelation coefficient – are independent on the locations. In Eq. (15), $\bar{\sigma}_t$ is then considered equal to $\bar{\sigma}_{t,S}$ (MAP estimate) rather than to $\bar{\sigma}_{t,x_0}$ (point estimate). One of the goal of the validation of the error AR model will therefore also be to verify the stability of ρ. Other rainfall estimation error models taking into account the dependence in time have been suggested (Retnam and Williams, 1988; Andrieu et al., 2003), but the proposed MAP estimation error model has the advantage to be simple, robust and suited to the observed data as will be shown in the coming section.

4 Step-by-step validation of this error model: example on the upper Loire river area

4.1 Validation of hourly precipitation error model

The validation of the kriging interpolation model has two objectives: (a) first to verify if the interpolated values can be considered as satisfactory and especially if they appear to be unbiased and (b) to verify the theoretical interpolation normalised error model. The related questions are the followings: Are the observed estimation error variances consistent with the theoretical variances? Are the distributions of the interpolation errors well approximated by Gaussian distributions with zero mean? In other word, are these distributions fully determined by their standard deviation $\bar{\sigma}$?

Empirical point rainfall interpolation error at point x_0 for the time step t can be defined as the difference between $\widehat{P}_t(x_0)$, the estimated value at this point based on interpola-

tion of values of the surrounding raingauges using the chosen variogram and $P_t(x_0)$, the "real" (measured if there is a raingauge, unknown if not) value of precipitation at this point x_0 and at the time t.

A cross-validation approach was first conducted to check the consistency between
5 theoretical (i.e. given by proposed error model) and observed (i.e. difference between measured and interpolated rainfall rate values) hourly point rainfall estimation normalised error standard deviations. It consists in removing in turn one raingauge from the network to compare the measured and interpolated rain rates at this specific site. Then, the distribution of theoretical errors (obtained from error model) can be com-
10 pared with the distributions of empirical errors (differences between observations and computed values). The validation can only be performed for point rainfall estimates, i.e. the only estimates for which reference values (observations) are available for the computation of estimation errors. This point cross-validation was carried out on the 40 raingauges available on this area.

15 A MAP is an weighted average of the linearly correlated point rainfall estimates. Therefore, if the hourly point rainfall estimation errors appear to follow a zero-mean Gaussian law with the theoretical kriging standard deviation at any location of the considered area, the hourly MAP estimation errors will also follow a zero-mean Gaussian law with the theoretical kriging standard deviation.

20 Table 2 and Fig. 4 compare the theoretical zero-mean Gaussian normalised error distributions and the observed hourly normalised rainfall interpolation error distributions for four validation raingauges, distributed over the upper Loire river catchment area. First, a relatively good adequacy between empirical and theoretical distributions can be observed. The results obtained for other gauges and for other periods – i.e.
25 other raingauge network structures, with a different $\bar{\sigma}$ – are similar. It confirms that the selected range of the variogram is well suited to the upper Loire river area and that the observed normalised error distributions can be well approximated by a zero-mean, Gaussian type distribution. Large normalised error values, especially negative errors corresponding to an underestimation of the rainfall intensity, are nevertheless

over-represented in the empirical validation set if compared to the theoretical Gaussian distribution. This is particularly noticeable in Table 2, where proportions of values comprised in the theoretical confidence intervals appear to be lower than the theoretical proportions. This is a common feature of rainfall interpolation techniques that smooth the rainfall fields and tend to underestimate extreme local values (Fig. 5).

Considering the simplicity of the interpolation model (linear interpolation with one parameter which is the variogram range) and of the error model (Gaussian error distributions), the validation results, still far from perfect, are nevertheless satisfactory. Of course, the consistency between observed and theoretical point rainfall estimation normalised errors is never perfect. But a good agreement at every validation gauge will ensure that the theoretical MAP Gaussian normalised error model will deliver realistic error ranges and distributions. The higher density of largely underestimated values in the observed distributions, if compared to the theoretical Gaussian one, explains both the bias and the higher standard deviation of the empirical error distributions. Overall, the Gaussian theoretical interpolation error model gives a reliable image of the kriging error distributions for interpolated hourly rain rates. It slightly underestimates the error ranges and percentiles and hence will lead to underestimate the effect of these errors on RR model outputs.

4.2 Validation of temporal dependence model

The simplest way to check if time dependence is correctly accounted for by the proposed model consists in comparing theoretical (simulated) and observed (empirical) estimation errors for rainfall amounts cumulated over several time steps. As far as the temporal dependence model is concerned, the first objective of the cross-validation is a comparison of theoretical and observed estimation error distributions for point rainfall amounts cumulated over a large range of time steps with an autocorrelation coefficient ρ adjusted for each location. The second objective is the verification that this coefficient ρ is not too much dependent on the location in order to be able to extrapolate the model to MAP errors.

Impact on streamflow simulations of uncertainties on MAP

L. Moulin et al.

Title Page

Abstract | Introduction

Conclusions | References

Tables | Figures

|◄ | ►|

◄ | ►

Back | Close

Full Screen / Esc

Printer-friendly Version

Interactive Discussion

The distributions of modelled and empirical normalised interpolation errors for rainfall amounts, cumulated over various time steps, are first compared to adjust the correlation coefficient and assess the reliability of the proposed temporal dependence model. Such a comparison is shown in Fig. 6 for the Machabert validation raingauge. Monte Carlo runs based on Eq. (15) are used to simulate series of hourly rain rate interpolation errors and then to build their distribution for various accumulation durations. The impact of the correlation coefficient on the error series structure and especially on the error distributions of rainfall amounts cumulated over more than one hour is clearly noticeable in Fig. 6. The comparison with the distributions of observed errors clearly reveals the necessity of taking into account the time-dependence of interpolation errors and the adequacy of the proposed time-dependence model. This adequacy is confirmed for other validation raingauges (Table 3). In most cases, the proposed model reproduces the evolution of the interpolation error distributions for rainfall amounts cumulated over a large range of time steps and for various locations of the raingauge network (not shown). Moreover, the correlation coefficient appears not to be too much dependent on the location in space, which is another very positive result of this cross-validation. Even if far from perfect, the proposed error model appears to be able to generate reliable point rainfall estimation error series. Although it could not be directly verified, according to the properties of the model presented in the previous section and to the stability of the temporal correlation coefficient, it can be assume that the proposed model certainly also provides reliable MAP estimation error series. The selected constant correlation coefficient (0.6) has been adjusted to slightly underestimate the quantiles of the error distributions at all the validation sites (Table 3). The error model will have a general tendency to underestimate the rainfall estimation errors and hence their effects on RR simulations.

5 Propagation of rainfall uncertainties through rainfall-runoff models

The interpolation error model is now selected and at least verified on point values –
since its validity for MAP could not be completely tested. Monte Carlo runs are now
implemented to simulate different scenarios of possible hourly MAP series correspond-
ing to the available point rainfall measurements. These scenarios are then propagated
into calibrated RR models to evaluate the impact of rainfall estimation uncertainties on
RR simulation results and hence on RR modelling efficiency.

5.1 Methodology

5.1.1 Rainfall-runoff modelling

The choice of adapted RR models is not the focus of the present study. A large body of
scientific literature has been devoted to this question. Most of the authors came to the
conclusion that the data sets routinely available in hydrology support the development
of models with only limited complexity – i.e. the calibration of models with a limited
number of parameters, typically 4 to 8 (Jakeman and Hornberger, 1993; Perrin et al.,
2001).

For these reasons, it has been decided to use robust lumped conceptual RR models
run on a continuous basis. According to both the available rainfall data and to the time
to peak of the considered catchments – between 3 and 18 h –, an hourly time step was
selected for the computations. An automatic local optimisation multi-start algorithm is
used for the calibration of the models (Edijatno et al., 1999; Mathevet, 2005). It is based
on a gradient search procedure to evolve step by step in the parameter space towards
the optimum parameter values, corresponding to a maximisation of the objective func-
tion used. The selected objective function is the standard Nash and Sutcliffe (1970)
efficiency on streamflow values (Eq. 16). A split sample test procedure (Klemeš, 1986)
is used to evaluate the performances of the models. The test consists in dividing the
total period of the available data set into sub-sets. One is used for the calibration of the

HESSD

5, 2067–2110, 2008

Impact on streamflow simulations of uncertainties on MAP

L. Moulin et al.

Title Page

Abstract	Introduction
Conclusions	References
Tables	Figures

◄◄	►►
◄	►
Back	Close

Full Screen / Esc

Printer-friendly Version

Interactive Discussion

parameters and the others for the evaluation of the model performances in a validation mode. The periods can be exchanged to multiply the number of validation tests. The Nash and Sutcliffe efficiencies obtained on the validation data sets are considered in order to evaluate the performances of the models.

$$\text{NSE} = 1 - \frac{\sum_{i=1}^{n}(Q_S(t_i) - Q_o(t_i))^2}{\sum_{i=1}^{n}(Q_o(t_i) - \bar{Q}_o(t_i))^2} \tag{16}$$

where $Q_s(t_i)$ and $Q_o(t_i)$ are the simulated and observed streamflows at time step i, n is the number of time steps in the period, and $\bar{Q}_o(t_i)$ is the mean observed streamflow during this period. This Nash-Sutcliffe efficiency criterion takes its values in the interval $[-\infty, 1]$.

The four-parameter GR4J model and the modified eight-parameter TOPMO model (Perrin et al., 2003; Mathevet, 2005) based on Topmodel (Beven and Kirby, 1979), have been selected to study the influence of MAP interpolation uncertainties. A comparison with other RR models on the upper Loire river data set has shown that these two models had on average the best performances (Moulin, 2007).

5.1.2   Simulated rainfall scenarios and their properties

To assess the impact of MAP uncertainties on streamflow simulations, Monte-Carlo simulations were conducted: 100 "possible" scenarios of MAP were generated with the above defined time-dependent error model for MAPs. These scenarios were then used as input for the RR models. Figure 7 presents the ranked highest simulated MAP errors for each of the 100 scenarios. The range and statistical distributions of these errors appear to vary depending on the catchment, and especially on its area, in a complex way linked both to the spatial and temporal dependencies and to the structure of the raingauge network. The maximum simulated MAPs and hence MAP error values affect the smaller catchments as illustrated in Figs. 7 and 8. This is due to the smoothing effect related to averaging that increases as the catchment area grows and tends to

reduce the variance of the computed MAPs. Another important and less obvious result appears on Fig. 8: the relative errors (divided by either measured or median values) on estimated hourly MAPs have a tendency to increase with the catchment areas. The ratio between the maximum computed MAP (about 50 mm/h) at Rieutord and the width of its estimated 90% confidence interval (about 20 mm/h) is of 40%. It is close to 50% for the Chambon-sur-Lignon catchment (respectively 28 mm/h and 14 mm/h) and to 100% for the Bas-en-Basset catchment (respectively 18 mm/h and 18 mm/h). This tendency is observed for all the MAP quantiles. To summarise, absolute errors on MAPs decrease while relative errors on MAPs increase when the considered area increases. Apparently MAP errors are less affected by the smoothing effect due to averaging than the MAPs themselves.

The consequences on simulated peak streamflows are difficult to anticipate and will therefore be tested trough numerical simulations. If the RR models were linear and if the RR relation was independent on the scale, the results would be similar for simulated streamflow relative errors (i.e. higher relative errors for larger catchments). But the RR relation is non-linear; its smoothing or amplification effect on input errors may depend on the absolute values of the MAPs which vary with the catchment size. Moreover, the RR relation depends on the catchment size and especially on the time of concentration of the catchment. The RR smoothing effect has a general tendency to increase with the area of the catchment since the streamflows result from an averaging of a larger amount of local processes over a longer period of time.

5.1.3 Impact assessment of MAP scenarios propagation in RR models

The 100 MAP scenarios were propagated into the two calibrated RR models for the three test catchments. A particular attention has been drawn to the width of the simulated streamflow uncertainty ranges in the analysis of the results. A specific criterion has been used to measure the sharpness of the streamflow simulation: the root mean square range criterion (RMSR, Eq. 17) between predefined percentiles of rainfall or

streamflow scenarios distribution.

$$\text{RMSR}(80\%) = \frac{1}{n} \sum_{i=1}^{n} \sqrt{(X_{90}(t_i) - X_{10}(t_i))^2} \qquad (17)$$

where RMSR(80%) is the criterion on the variable X (precipitation or streamflow) for the confidence interval 80%, n is the number of the time step, and $X_{10}(t_i)$ and $X_{90}(t_i)$ are the percentiles 10% and 90% of the variable X for the time t_i. As a complement, the standard Nash and Sutcliffe criterion between percentile 50% and measured values (Eq. 16) give an estimation of accuracy on the estimates.

5.2 Results and discussion: impact on streamflow simulations

5.2.1 Sharpness of RR simulations

For each of the three catchments, the RMSR value was computed for both rainfall and streamflow series, and for various confidence intervals (Table 4). When comparing RMSR on streamflows (in mm/h) with RMSR on precipitation (in mm/h), it appears that this ratio increases with decreasing catchment areas: RMSR on streamflow represent roughly 28% of RMSR on precipitation for the catchment of the Loire at Rieutord (62 km^2), 15% for the Lignon at Chambon-sur-Lignon (139 km^2) and around 7% for the Loire River at Bas-en-Basset (3234 km^2). There is roughly no difference in sharpness between the two tested RR models.

This confirms the foreseen higher smoothing effect of the RR process for large catchments – at least, simulated by the RR models. As shown in Fig. 9, the 90% relative confidence intervals on simulated streamflows do not appear to depend anymore on the catchment: the ratio between the width of the confidence interval and the simulated streamflow values is stable and close to 50%. As a first conclusion of the MAP uncertainty propagation exercise, it comes out that, for different reasons, uncertainties in MAP estimations equally affect streamflow simulations independently of the catchment area.

5.2.2 Accuracy of RR simulations

Overall, the computed 90% confidence intervals on simulated streamflow series are large. These confidence intervals have been reported on Fig. 10, along with both the measured hydrographs and the ranges of the simulated hydrographs for one of the major flood events in the record period for the upper Loire river area. The impact of the MAP uncertainties on the streamflow simulations appears to be dramatic. The upper bound of the 90% simulated confidence interval is about 1.5 times higher than the lower bound. Even if the RR models were perfect, which they are of course far from, MAP estimation uncertainties set a relatively low limit to the accuracy of streamflow simulations or forecasts. Moreover, the measured hydrograph appears to be contained in, or very close to, the 90% confidence interval for the two examples presented in Fig. 10: i.e. the distance between simulated and measured hydrographs may be explained by errors in the estimation of MAPs. Similar observations are made for all the catchments and simulated streamflow series.

Table 5 gives the proportion of measured streamflows comprised in the computed 90% confidence limits for the whole test period (20–27 years) and the three catchments. A large proportion of measured streamflows appears to be comprised in this confidence interval. This is particularly true during severe flood events (observed streamflow greater than 10 times the mean annual streamflow) and when a tolerance of plus or minus 20% is considered for the measured streamflows. This tolerance stands for both the streamflow measurement uncertainties and the level of efficiency of RR models expected by operational forecasters. For the smallest catchments (Rieutord, Chambon-sur-Lignon), the simulated 90% confidence interval contains almost 90% of the measured streamflow values when a tolerance factor of 20% is considered (Table 5). In other words, rainfall estimation uncertainties may explain a large part of the differences between measured and simulated streamflows. Rainfall estimation uncertainties appear in this case as a major factor limiting the accuracy of streamflow simulations. Conversely, according to the existing uncertainties on estimated MAPs and

their impact on RR simulations, RR simulation accuracy will hardly be improved without a significant reduction of the MAP estimation errors. This pleads for an improvement of the rainfall measurement networks and techniques.

For the larger catchment of the Loire river at Bas-en-Basset, uncertainties on MAP are nevertheless far from explaining all of the RR modelling errors. In this last case, other error sources seem to affect significantly the RR simulations. A detailed analysis of the simulated and observed hydrographs reveals delays and apparent fluctuations of both the runoff rates and the times-to-peak between events. That undoubtedly can be attributed, to a great extent, to the spatial repartition of the rainfall. Higher runoff rates are generally observed during convective events when the rainfall is concentrated on a limited part of the catchment if compared to stratiform events with a homogeneous rainfall repartition. Likewise, the time-to-peak depends on the location of the rain cells on the catchment and their distance from the outlet for convective rainfall events. The tested lumped modelling approach becomes here limited. For larger catchment areas, according to the results presented herein, the use of distributed or semi-distributed hydrological models might bring some improvements to the RR simulations. Nevertheless, this possible gain should be put into perspective by considering the number of calibrated parameters: problems as over-parametrisation might emerge.

As a conclusion to this MAP uncertainty propagation excercise, a large part of the streamflow simulation errors may be attributed to MAP estimation errors, except on large catchments (typically areas over $500\,\mathrm{km}^2$) where the shape of the hydrograph can be influenced by the spatio-temporal pattern of the rainfall event, and where a spatialised modelling approach might bring improvement if compared to the tested lumped models. Even if the RR models were perfect, MAP estimation uncertainties are clearly a major constraint on both accuracy and sharpness of stream flow simulations or forecasts.

6   Summary and conclusions

The objective of this study was twofold: to propose a reliable estimate of MAP uncertainties when MAPs are obtained through the interpolation of raingauge measurements and investigate the possible impact of MAP estimation errors on RR simulations.

If compared with previous published results on the same issue, the main originality of this study lies in the development and partial validation of a reliable error model (consistent with data) to represent uncertainties on MAP. Whereas most of the previous studies use either completely empirical error estimations or a priori error models, we propose a time-dependent error model based on geostatistics and validated to the greatest possible extent.

Monte Carlo simulations based on this error model reveal that uncertainties on MAP estimations induce large uncertainties in RR simulations. For different reasons, all the tested catchments are equally affected by this phenomenon: the relative size of the computed confidence interval is independent on the catchment area. The higher relative error values on MAPs are compensated by a higher smoothing effect of the RR transformation when larger catchment areas are considered.

The comparison with measured streamflows shows that a large part of the lumped RR simulation errors may be explained by the uncertainties on MAP estimations. This is particularly true for the two smallest catchments studied, whereas on the larger catchment the shape of the hydrograph can be influenced by the spatio-temporal pattern of the rainfall event and distributed RR models may bring an improvement if compared to the tested lumped models. This implies that for a certain range of catchment areas (up a few hundred square kilometers), MAP estimation uncertainties drastically restrict the possible accuracy of streamflow simulations and set a limit to both future developments and improvements of RR models. Even in an optimal situation – good quality and long datasets, intensive effort for RR model selection and calibration – RR simulation errors can hardly be reduced without a significant improvement of the rainfall measurement networks and techniques.

From a practical point of view, operational forecasting services should be aware of these limits to efficiently use the RR models and if possible evaluate the RR simulation uncertainties in real time to be able to deliver confidence intervals along with their traditional deterministic forecasts. Ensemble or Monte Carlo forecasts are now used routinely in meteorological forecasting; there is no reason why they should be disregarded by hydrologists. The error scenario simulation model developed here could help to build such ensemble forecasts in the case where MAP amounts are estimated through a rain gauge network. The same type of model is still to be developed for the case where quantitative radar estimations are used.

References

Anctil, F., Lauzon, N., Andreassian, V., Oudin, L., and Perrin, C.: Improvement of rainfall-runoff forecasts through mean areal rainfall optimization, J. Hydrol., 328, 717–725, 2006. 2071

Andreassian, V., Hall, A., Chahinian, N., and Schaake, J.: Large Sample Basin Experiments for Hydrological Model Parameterization: Results of the Model Parameter Experiment – MOPEX, IAHS Publication, 307, 2006. 2068

Andrieu, H., French, M. N., Krajewski, W. F., and Georgakakos, K. P.: Stochastic-dynamical rainfall simulation based on weather radar volume scan data, Adv. Water Resour., 26, 581–593, 2003. 2079

Balme, M., Vischel, T., Lebel, T., Peugeot, C., and Galle, S.: Assessing the water balance in the Sahel: Impact of small scale rainfall variability on runoff: Part 1: Rainfall variability analysis, J. Hydrol., 331, 336–348, 2006. 2071

Bardossy, A. and Das, T.: Influence of rainfall observation network on model calibration and application, Hydrol. Earth Syst. Sci., 12, 77–89, 2008, http://www.hydrol-earth-syst-sci.net/12/77/2008/. 2069, 2071

Impact on streamflow simulations of uncertainties on MAP

L. Moulin et al.

Beven, K. and Kirby, M.: A physically-based, variable contributing area model of basin hydrology, Hydrol. Sci. B., 23, 419–438, 1979. 2071, 2084

Borga, M.: Accuracy of radar rainfall estimates for streamflow simulation, J. Hydrol., 267, 26–39, 2002. 2070

5   Borga, M., Degli Esposti, S., and Norbiato, D.: Influence of errors in radar rainfall estimates on hydrological modeling prediction uncertainty, Water Resour. Res., 42, W08409, doi:10.1029/2005WR00459, 2006. 2070

Carpenter, T. M. and Georgakakos, K. P.: Impacts of parametric and radar rainfall uncertainty on the ensemble streamflow simulations of a distributed hydrologic model, J. Hydrol., 298, 202–221, 2004. 2070, 2071

10

Carpenter, T. M., Georgakakos, K. P., and Sperfslagea, J. A.: On the parametric and NEXRAD-radar sensitivities of a distributed hydrologic model suitable for operational use, J. Hydrol., 253, 169–193, 2001. 2070

Chapon, B., Delrieu, G., Gosset, M., and Boudevillain, B.: Variability of rain drop size distribution and its effect on the Z-R relationship: A case study for intense Mediterranean rainfall, Atmos. Res., 87, 52–65, 2008. 2069

15

Chen, Y.-C., Wei, C., and Yeh, H.-C.: Rainfall network design using kriging and entropy, Hydrol. Processes, 22, 330–346, 2008. 2074

Cole, S. J. and Moore, R. J.: Hydrological modelling using raingauge- and radar-based estimators of areal rainfall, J. Hydrol., accepted, 2008. 2070

20

Creutin, J. and Obled, Ch.: Objectives analyses and mapping techniques for rainfall fields : an objective comparison, Water Resour. Res., 18, 413–431, 1982. 2070

Datin, R.: Outils opérationnels pour la prévision des crues rapides: traitements des incertitudes et intégration des prévisions météorologiques. Développements de TOPMODEL pour la prise en compte de la variabilité spatiale de la pluie. Application au bassin versant de l'Ardèche., Ph.D. thesis, Institut National Polytechnique de Grenoble, Grenoble, 369 pp., 1998. 2071

25

Delrieu, G.: The Cevennes-Vivarais Mediterranean Hydro-meteorological observatory, Houille Blanche, 6, 83–88, 2003. 2072

30   Delrieu, G., Ducrocq, V., Gaume, E., Nicol, J., Payrastre, O., Yates, E., Kirstetter, P. E., Andrieu, H., Ayral, P. A., Bouvier, C., Creutin, J. D., Livet, M., Anquetin, S., Lang, M., Neppel, L., Obled, C., Parent-du Chatelet, J., Saulnier, G. M., Walpersdorf, A., and Wobrock, W.: The catastrophic flash-flood event of 8–9 September 2002 in the Gard region, France: A first

Impact on streamflow simulations of uncertainties on MAP

L. Moulin et al.

Title Page

Abstract	Introduction
Conclusions	References
Tables	Figures

I◄	►I
◄	►
Back	Close

Full Screen / Esc

Printer-friendly Version

Interactive Discussion

case study for the Cevennes-Vivarais Mediterranean Hydrometeorological Observatory, J. Hydrometeorol., 6, 34–52, 2005. 2072

Dulal, K., Takeuchi, K., and Ishidaira, H.: A framework for the Analysis of Uncertainty in the Measurement of Precipitation Data: a case study for Nepal., in: Agricultural Engineering International: the CIGR E-journal, Manuscript LW 06 100. vol VIII., 2006. 2070

Edijatno, Nascimento, N., Yang, X., Makhlouf, Z., and Michel, C.: GR3J: a daily watershed model with three free parameters, Hydrol. Sci. J., 44(2), 263–277, 1999. 2083

Gourley, J. J. and Vieux, B. E.: A method for identifying sources of model uncertainty in rainfall-runoff simulations, J. Hydrol., 327(1–2), 68–80, 2006. 2069

Haberlandt, U.: Geostatistical interpolation of hourly precipitation from rain gauges and radar for a large-scale extreme rainfall event, J. Hydrol., 332, 144–157, 2007. 2073, 2074

Jakeman, A. and Hornberger, G.: How much complexity is warranted in a rainfall-runoff model?, Water Resour. Res., 29(8), 2637–2649, 1993. 2083

Johansson, B.: Areal precipitation and temperature in the Swedish mountain. An evaluation from a hydrological perspective., Nord. Hydrol., 31, 207–228, 2000. 2071

Kieffer-Weisse, A. and Bois, P.: A comparison of methods for mapping statistical characteristics of heavy rainfall in the French Alps: the use of daily information, Hydrol. Sci. J., 47(5), 739–752, 2002. 2074

Klemeš, V.: Operationnal testing of hydrological simulation models, Hydrol. Sci. J., 31(1), 13–24, 1986. 2083

Krajewski, W. F. and Smith, J.: Radar hydrology: rainfall estimation., Adv. Water Resour., 25(8-12), 1387–1394, 2002. 2069

Lebel, T., Bastin, G., Obled, Ch., and Creutin, J.: On the accuracy of areal rainfall estimation : a case study., Water Resour. Res., 23, 2123–2134, 1987. 2071, 2073, 2074, 2075, 2076

Mathevet, T.: Quels modèles pluie-debit globaux au pas de temps horaire? Développements empiriques et intercomparaison de modèles sur un large échantillon de bassins versants., Ph.D. thesis, ENGREF, 463 pp., 2005. 2071, 2083, 2084

Melching, C.: Computer Models of Watershed Hydrology, Chap. 3. Reliability estimation, pp. 69–118, 1995. 2069

Michaud, J. and Sorooshian, S.: Comparison of simple versus complex distributed runoff models on a midsized semiarid watershed, Water Resour. Res., 30, 593–605, 1994. 2069

Moulin, L.: Prévision des crues rapides avec des modèles hydrologiques globaux. Application aux bassins opérationnels de la Loire supérieure: évaluation des modélisations, prise en

Impact on streamflow simulations of uncertainties on MAP

L. Moulin et al.

compte des incertitudes sur les précipitations moyennes spatiales et utilisation de prvisions météotorologiques., Ph.D. thesis, ENGREF, 643 pp., 2007. 2084

Nandakumar, N. and Mein, R. G.: Uncertainty in rainfall–runoff model simulations and the implications for predicting the hydrologic effects of land-use change, J. Hydrol., 192, 211–232, 1997. 2071

Nash, J. and Sutcliffe, J.: River flow forecasting through conceptual models. Part I – A discussion of principles., J. Hydrol., 10(3), 282–290, 1970. 2083

Oudin, L., Perrin, C., Mathevet, T., Andreassian, V., and Michel, C.: Impact of biased and randomly corrupted inputs on the efficiency and the parameters of watershed models, J. Hydrol., 320, 62–83, 2006. 2071

Paturel, J. E., Servat, E., and Vassiliadis, A.: Sensitivity of conceptual rainfall-runoff algorithms to errors in input data – case of the GR2M model, J. Hydrol., 168, 111–125, 1995. 2071

Perrin, C., Michel, C., and Andreassian, V.: Does a large number of parameters enhance model performance? Comparative assessment of common catchment model structures on 429 catchments, J. Hydrol., 242, 275–301, 2001. 2083

Perrin, C., Michel, C., and Andrassian, V.: Improvement of a parsimonious model for streamflow simulation, J. Hydrol., 279, 275–289, 2003. 2071, 2084

Refsgaard, J. C., van der Sluijs, J. P., Brown, J., and van der Keur, P.: A framework for dealing with uncertainty due to model structure error, Adv. Water Resour., 29, 1586–1597, 2006. 2070

Retnam, M. T. P. and Williams, B. J.: Input errors in rainfall-runoff modelling, Math. Comput. Simulat., 30, 119–131, 1988. 2079

Rode, M. and Suhr, U.: Uncertainties in selected river water quality data, Hydrol. Earth Syst. Sci., 11, 863–874, 2007, http://www.hydrol-earth-syst-sci.net/11/863/2007/. 2070

Segond, M. L., Wheater, H. S., and Onof, C.: The significance of spatial rainfall representation for flood runoff estimation: A numerical evaluation based on the Lee catchment, UK, J. Hydrol., 347, 116–131, 2007. 2069

Storm, B., Jensen, K. H., and Refsgaard, J. C.: Estimation of catchment rainfall uncertainty and its influence on runoff prediction, Nord. Hydrol., 19, 77–88, 1989. 2071

Sun, X., Mein, R. G., Keenan, T. D., and Elliott, J. F.: Flood estimation using radar and raingauge data, J. Hydrol., 239, 4–18, 2000. 2069

Villarini, G., Mandapaka, P., Krajewski, W., and Moore, R.: Rainfall and sampling uncertainties:

Impact on streamflow simulations of uncertainties on MAP

L. Moulin et al.

A rain gauge perspective., J. Geophys. Res., 113, D11102, doi:10.1029/2007JD009214, 2008. 2070, 2078

Vischel, T. and Lebel, T.: Assessing the water balance in the Sahel: Impact of small scale rainfall variability on runoff. Part 2: Idealized modeling of runoff sensitivity, J. Hydrol., 333, 340–355, 2007. 2069

Xu, C. Y. and Vandewiele, G. L.: Sensitivity of monthly rainfall-runoff models to input errors and data length, Hydrol. Sci. J., 39, 157–176, 1994. 2071

Impact on streamflow simulations of uncertainties on MAP

L. Moulin et al.

Title Page

Abstract | Introduction

Conclusions | References

Tables | Figures

◄ | ►

◄ | ►

Back | Close

Full Screen / Esc

Printer-friendly Version

Interactive Discussion

Table 1. Main hydroclimatic characteristics of the three studied catchments ($\bar{P}$: mean annual precipitation; $\bar{Q}$: mean annual flow; Q_{10}: decennial flow).

River	Drainage area (km^2)	Period of record	$\bar{P}$ (mm/y)	$\bar{Q}$ (mm/y,[m^3/s])	$\bar{P}/\bar{Q}$	Q_{10} (m^3/s/km^2)
Loire at Rieutord	62	1983–2002	1530	1420 [2.7]	0.90	5.6
Lignon at Chambon	139	1977–2003	945	726 [3.2]	0.77	1.4
Loire at Bas-en-Basset	3234	1977–2003	900	364 [37.3]	0.40	0.4

Title Page

Abstract   Introduction

Conclusions   References

Tables   Figures

|◄   ►|

◄   ►

Back   Close

Full Screen / Esc

Printer-friendly Version

Interactive Discussion

Table 2. Percentage of computed interpolation errors comprised in various theoretical confidence intervals for four raingauges.

Raingauge	68% CI ($\pm\sigma$)	95% CI ($\pm2\sigma$)	99.7% CI ($\pm3\sigma$)
Fay	53.5	77.3	89.8
Goudet	59.4	80.7	90.3
Machabert	63.1	84.8	93.4
Mazet	59.8	81.8	91.0
Theoretical value	68.0	95.0	99.7

Table 3. Standard deviations of the empirical normalised error on mean intensities over various durations: observed (normalised errors obtained with the cross validation) and simulated with time-dependent error model. A constant correlation coefficient is equal to 0.6.

Time step (hours)	Fay Obs.	Fay Sim.	Goudet Obs.	Goudet Sim.	Machabert Obs.	Machabert Sim.	Mazet Obs.	Mazet Sim.
1	1.05	0.74	0.76	0.66	0.76	0.77	0.97	0.69
2	0.95	0.65	0.66	0.58	0.69	0.68	0.72	0.61
4	0.79	0.54	0.55	0.49	0.55	0.56	0.57	0.51
6	0.70	0.47	0.49	0.42	0.48	0.49	0.47	0.44
12	0.58	0.36	0.39	0.33	0.40	0.38	0.36	0.34
24	0.49	0.26	0.29	0.24	0.32	0.27	0.28	0.24

Table 4. Root mean square range (RMSR) of hourly precipitation (P in mm/h) and on streamflow (Q in mm/h) scenarios as a measure of uncertainty.

			50%	80%	90%	95%	100%	Ratio Q/P
Rieutord	P		0.278	0.514	0.644	0.749	0.982	
Rieutord	Q	GR4J	0.078	0.148	0.186	0.217	0.279	≈28%
Rieutord	Q	TOPM	0.076	0.145	0.182	0.212	0.275	≈28%
Chambon	P		0.244	0.433	0.536	0.619	0.794	
Chambon	Q	GR4J	0.036	0.067	0.085	0.097	0.126	≈15%
Chambon	Q	TOPM	0.037	0.068	0.085	0.098	0.126	≈15%
Bas-en-Basset	P		0.194	0.360	0.447	0.515	0.660	
Bas-en-Basset	Q	GR4J	0.012	0.024	0.030	0.038	0.051	≈7%
Bas-en-Basset	Q	TOPM	0.011	0.022	0.028	0.035	0.044	≈7%

Table 5. Proportion (in %) of the observed values comprised in the 90% simulated confidence interval, with and without a 20% tolerance on observed streamflow values (in [ ] in case of a tolerance of 20% but without taking into account uncertainties on MAP). $\bar{Q}$ is the mean stream-flow; Q_{10} is an estimate of the decennial streamflow.

	Rieutord			Chambon			Bas-en-Basset		
	Qobs	Qobs ±20%		Qobs	Qobs ±20%		Qobs	Qobs ±20%	
All data	22.2	55.3	[39.0]	18.6	42.0	[24.2]	10.9	28.0	[15.4]
$Q_{obs}>10\bar{Q}$	34.2	68.7	[42.0]	28.4	53.6	[24.7]	21.9	50.6	[28.9]
$Q_{obs}>Q_{10}$	66.7	100.0	[33.0]	47.5	65.0	[40.0]	77.8	88.9	[33.3]
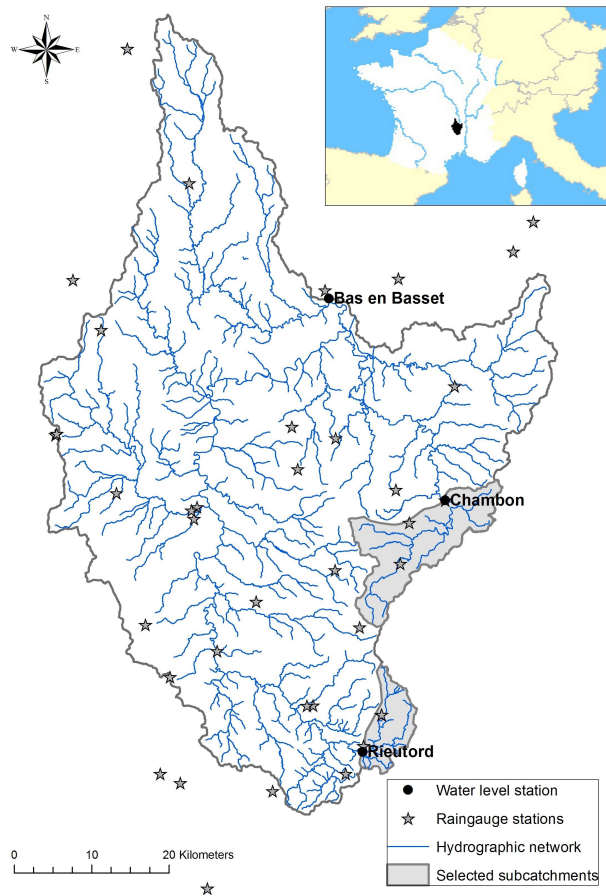
Fig. 1. The upper Loire river catchment at Bas-en-Basset (3234 km^2) with two subcatchments shown in gray: the Loire river at Rieutord (62 km^2) and the Lignon river at Chambon-sur-Lignon (139 km^2). Raingauges stations indicated correspond to the hourly network available in 2003.

Full Screen / Esc
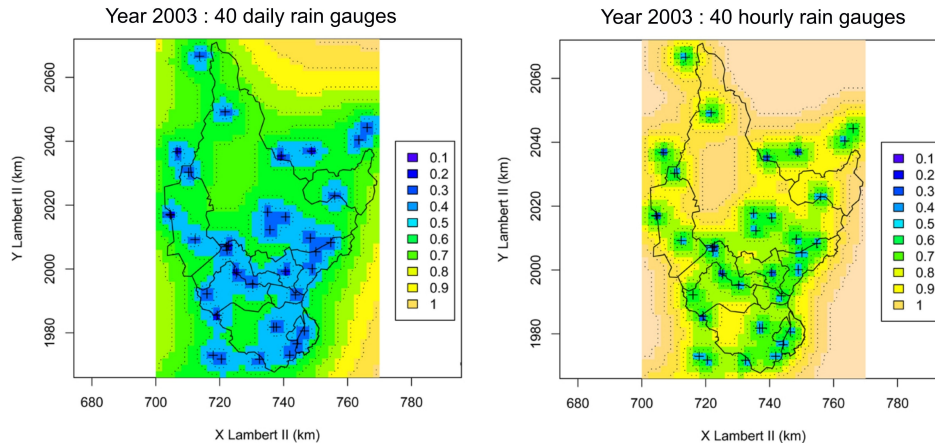
Fig. 2. Maps of theoretical normalised kriging standard deviation ($\bar{\sigma}$) for the network over the upper Loire river catchment area available in 2003 and for two time step: daily time step (left) and hourly time step (right).
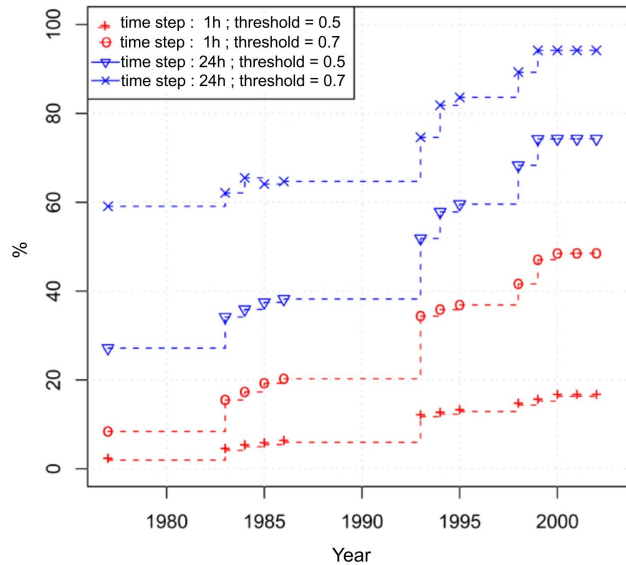
Fig. 3. Evolution of the percentage of the upper Loire river area where the theoretical normalised kriging standard deviation is lower than 0.5 (75% of variance is explained) or 0.7 (50% of variance is explained) for the cases of both dayly and hourly time step.
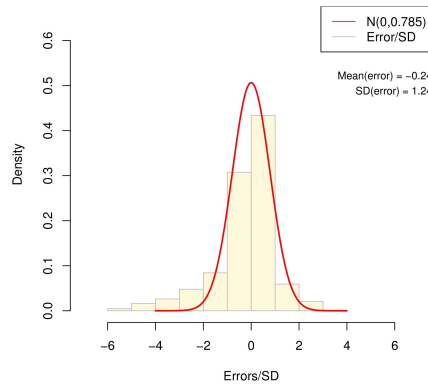
Fig. 4. Comparison between the distributions of theoretical and empirical (obtained with cross-validation and represented as histograms) normalised rainfall estimation errors for four rain gauges of the network.
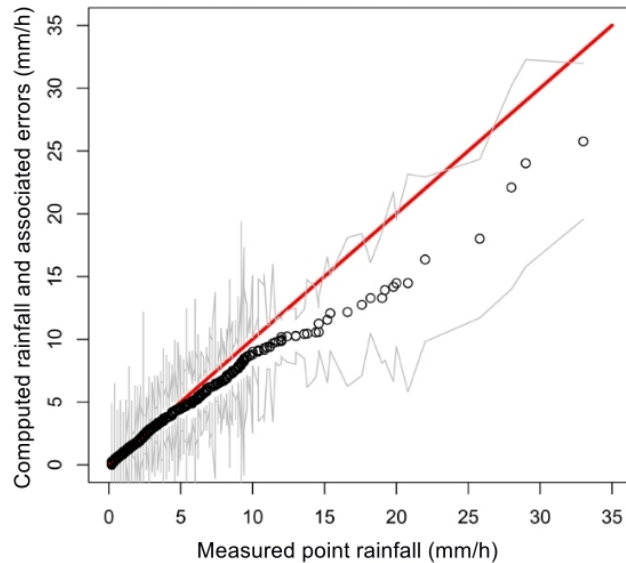
Fig. 5. Point hourly precipitations ranked in ascending order versus corresponding interpolated values (cross validation) and associated errors (from the proposed Gaussian error model) at Mazet rain gauge.
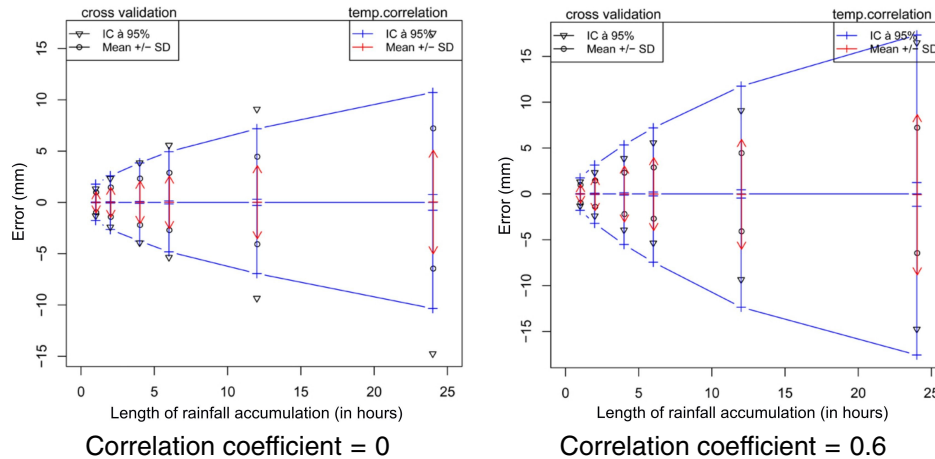
Fig. 6. Comparison between observed (crosses and triangles) and simulated (lines) interpolation error quantiles for rainfall accumulations over 1 to 24 h at Machabert (left: no temporal dependence; right: temporal dependence with a correlation of 0.6).
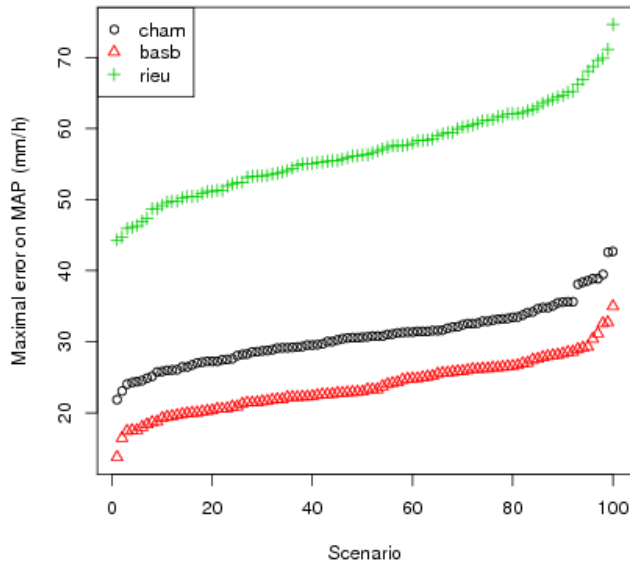
Fig. 7. Distribution of higher errors on MAP generated for each one of 100 scenarios and for each one of the three catchments of upper Loire river (rieu = Rieutord $(62\,km^2)$; cham = Chambon-sur-Lignon $(139\,km^2)$; basb = Bas-en-Basset $(3234\,km^2)$; flood of 11 November 1996).

Rieutord (62 km^2)   Chambon (139 km^2)   Bas-en-Basset (3234 km^2)
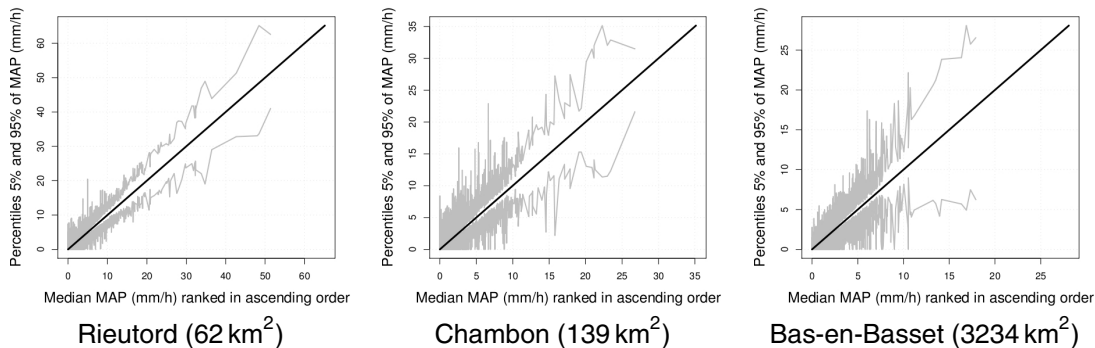
Fig. 8. Percentiles of uncertainty on MAP for Rieutord (left), Chambon-sur-Lignon (center) and Bas-en-Basset (right).

Rieutord (62 km^2)   Chambon (139 km^2)   Bas-en-Basset (3234 km^2)
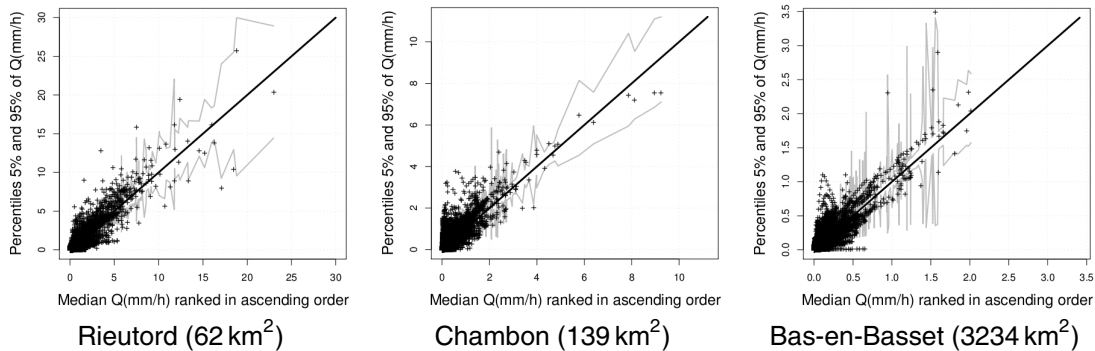
Fig. 9. Percentiles of uncertainty on streamflow (mm/h) for Rieutord (left), Chambon-sur-Lignon (center) and Bas-en-Basset (right). "+" indicate measured values versus median of simulated values.
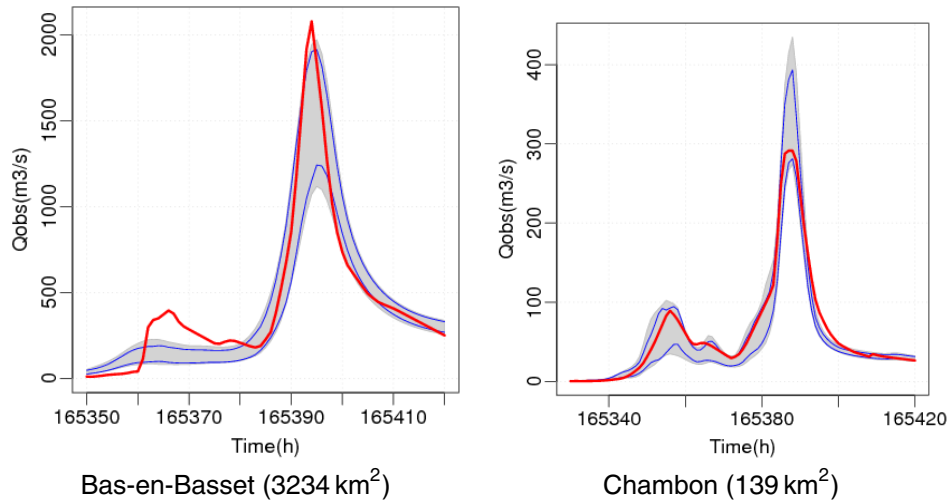
Fig. 10. Two examples of observed flood hydrographs (black lines), 90% confidence interval for the simulated streamflow (grey lines) and limits of the simulated streamflow values obtained after 20 Monte carlo runs. Flood of 11 November 1996 at Bas-en-Basset (3234 km^2, left) and Chambon-sur-Lignon (139 km^2, right).
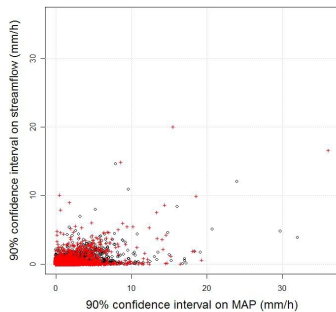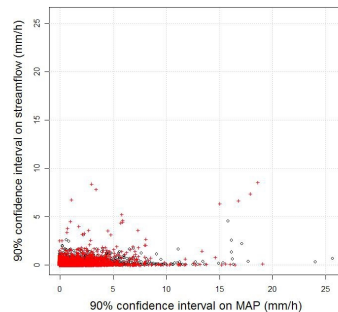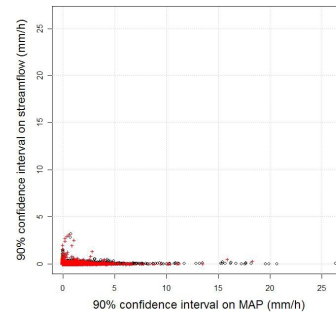
Rieutord (62 km^2): 22%   Chambon (139 km^2): 19%   Bas-en-Basset (3234 km^2): 11%

Fig. 11. Relation between uncertainty on MAP and uncertainty on streamflow. "+" indicates cases where observed streamflow is comprised in 90% confidence interval (percentages are indicated at the bottom of figures).